Role of Plk2 (Snk) in Mouse Development and Cell Proliferation

MOLECULAR AND CELLULAR BIOLOGY, Oct. 2003, p. 6936–6943 Vol. 23, No. 19
0270-7306/03/$08.00+0 DOI: 10.1128/MCB.23.19.6936–6943.2003

Role of *Plk2* (*Snk*) in Mouse Development and Cell Proliferation

Sheng Ma,[1] Jean Charron,[2] and Raymond L. Erikson[1]*

Department of Molecular and Cellular Biology, Harvard University, Cambridge, Massachusetts 02138,[1] and Centre de Recherche en Cancérologie de l'Université Laval, L'Hôtel-Dieu de Québec, CHUQ, Québec, Canada G1R 2J6[2]

Received 29 May 2003/Accepted 16 June 2003

Plk2 (Snk) is a polo-like kinase expressed at G_1 in cultured cells and mainly in the hippocampal neurons in the brains of adult rodents, but its function is poorly understood. We have generated mice deficient in Plk2 by gene targeting. Although Plk2 is not required for postnatal growth, *Plk2*$^{-/-}$ embryos show retarded growth and skeletal development late in gestation. The labyrinthine zone of the placenta is diminished in *Plk2*$^{-/-}$ embryos due to decreased cell proliferation. Cultured *Plk2*$^{-/-}$ embryonic fibroblasts grow more slowly than normal cells and show delayed entry into S phase. These data suggest a role for *Plk2* in the cell cycle.

The Plks have emerged as important regulators of the cell cycle. Plks are characterized by the presence of a conserved polo box at the C terminus, and their expression and activities are regulated during the cell cycle (19). One class of Plks which is conserved from yeast to human is highly expressed and active during G_2/M and is critical for the progression of mitosis. One of the functions of members of this class is to regulate the mitotic cyclin-dependent kinases (Cdks). Cyclin B1 is phosphorylated by Plk1 (55), and in *Xenopus* egg extracts, Plx1 phosphorylates Cdc25C and activates its phosphatase activity, resulting in the activation of Cdc2 (30, 42). Many other functions are also attributed to the mitotic Plks. They are required for the fragmentation of the Golgi apparatus (34, 52), as well as maturation and separation of centrosomes, during the G_2/M transition (10, 32, 35). The mitotic Plks are involved in the formation of the mitotic spindle and dissociation of cohesin from chromosomes in early M phase (32, 38, 40, 50, 51). During the metaphase-to-anaphase transition, mitotic Plks are involved in phosphorylation and activation of the anaphase-promoting complex and separation of sister chromatids (1, 15, 29, 45). Furthermore, mitotic Plks are required for completion of cytokinesis (2, 9, 49), since either depleting or elevating their kinase activity blocks complete separation of daughter cells (9, 33, 41). Studies also suggest that mitotic Plks are involved in DNA damage and the spindle checkpoints (23, 44, 48, 53), and a possible role in regulating DNA replication was reported for the sole Plk in budding yeast, Cdc5 (20).

Two additional Plks have been described in frog and mammalian cells. *Plk2* and *Plk3* (*Fnk*/*Prk*) were both identified as immediate-early transcripts in cultured murine fibroblasts (11, 47). Plk3 is expressed throughout the cell cycle, although its abundance increases from G_1 to M phase, and it appears to be phosphorylated in M phase (4). On the other hand, Plk2 expression is detected only in G_1, and endogenous Plk2 is rapidly turned over (36). Therefore, the expression of the three mammalian Plks during the cell cycle resembles the successive transition of the cyclins, prompting speculation that Plks may regulate the cell cycle in a manner analogous to that of Cdks (31). Although the role of Plk3 is not well characterized, there are reported functions for Plk3 in the cell cycle. For example, Plk3 phosphorylates and activates Cdc25C (39), and maturation of *Xenopus* oocytes was accelerated by microinjection of Plx3 mRNA and delayed by injection of a kinase-deficient mutant (12). Moreover, overexpression of Plk3 resulted in incomplete cytokinesis (5). Plk3 may also be involved in the DNA damage checkpoint, possibly through the p53 pathway (58). It is not clear, however, how some other reported functions of Plk3 fit into the cell cycle. One study suggested that Plk3 may be involved in cell adhesion in human macrophages (22), and the expression of Plk3 in rat brain appeared to correlate with neuronal activities (27). Recently, endogenous Plk3 was shown to localize to the centrosome, and overexpression of Plk3 induced changes in cell morphology (57).

Relatively few reports of the function of Plk2 have appeared. In the adult mouse, Plk2 expression is detected in the brain but not in proliferating tissues, such as the thymus or testis (47), and it was reported that the level of Plk2 in the brain is increased by stimuli that induce long-term potentiation (27). When ectopically expressed, Plk2 caused changes in cell morphology and, after an extended period of time, cell death (36). Plk2 was also shown to interact with the calcium- and integrin-binding protein CIB, which inhibits Plk2 kinase activity (36). Despite these data, the role of *Plk2*, and especially whether it is involved in the regulation of the cell cycle, remains elusive. To investigate the function of *Plk2* in vivo, we generated mouse lines carrying a null mutation in the *Plk2* gene. Analysis of the growth and development of *Plk2*$^{-/-}$ mice indicated that *Plk2* is involved in embryonic development and cell cycle progression.

MATERIALS AND METHODS

Gene replacement vector and gene targeting. A bacterial artificial chromosome (BAC) clone containing the *Plk2* locus was identified through Southern blot analysis of mouse embryonic stem (ES) cell 129/SvJ BAC high-density filters (Genome Systems, Inc., St. Louis, Mo.), using full-length *Plk2* cDNA as a probe. A 13-kbp *Bam*HI fragment was subcloned and completely sequenced, revealing 14 *Plk2* exons (Fig. 1A). A replacement vector was constructed by cloning a cassette encoding herpes simplex virus thymidine kinase into the *Sal*I and *Eco*RI sites of pBluescript KS(−) and a 6.6-kbp *Xba*I *Plk2* DNA fragment into the *Spe*I site. A 750-bp *Sal*I fragment containing half of the first exon and the entire second exon of *Plk2* was replaced with a 1.2-kbp Neo cassette. TC1 ES cells were handled as previously described (43). For electroporation, ES cells were

* Corresponding author. Mailing address: Department of Molecular and Cellular Biology, Harvard University, 16 Divinity Ave., Cambridge, MA 02138. Phone: (617) 495-5386. Fax: (617) 495-0681. E-mail: erikson@mcb.harvard.edu.

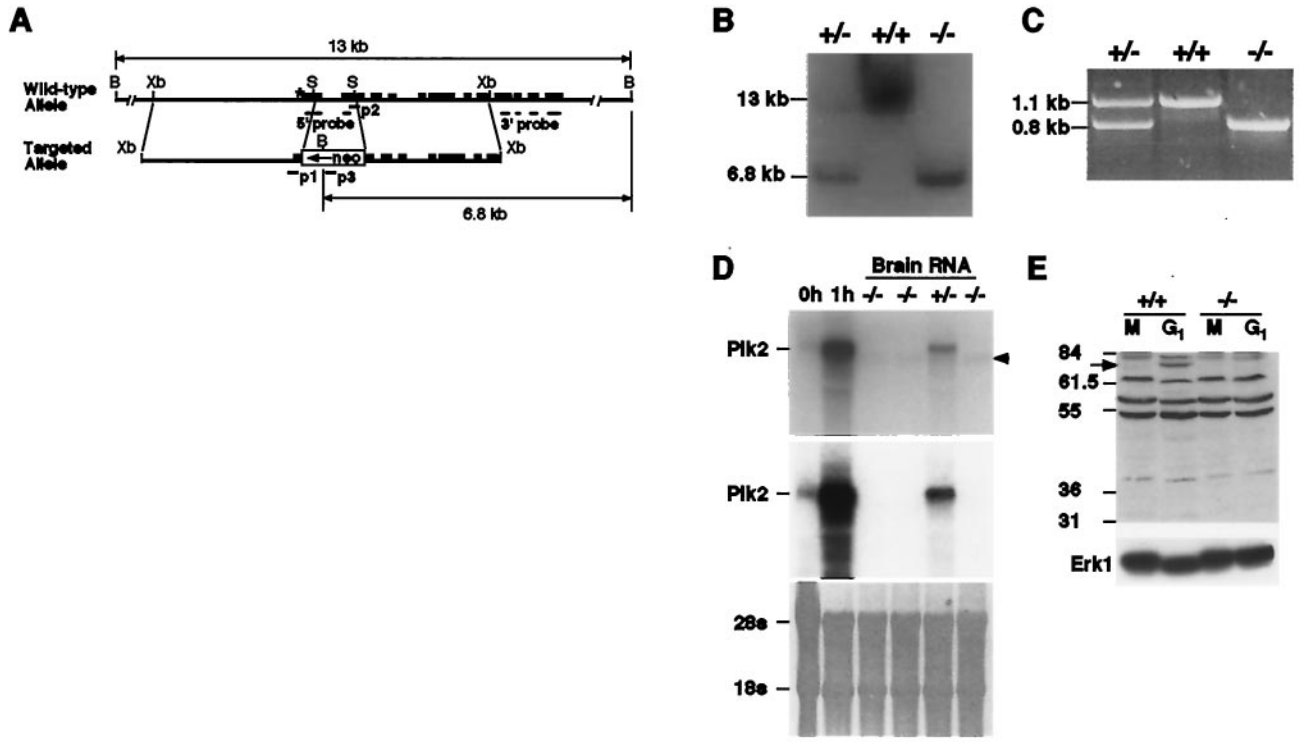

FIG. 1. Gene targeting of the *Plk2* locus. (A) Creation of a *Plk2* deletion allele. *Plk2* exons are indicated as solid boxes, with the asterisk indicating the first exon. The *Xba*I (Xb) fragment was cloned into a gene replacement vector, and the *Sal*I fragment was replaced by a Neo cassette. The positions of PCR primers (p1 to p3) and exons whose corresponding cDNA sequences (5′ and 3′ probes) were used as the probes in Southern and Northern blot analyses are indicated. B, *Bam*HI; S, *Sal*I. (B) Southern blot analysis showing the disruption of the *Plk2* locus. Genomic DNA was digested with *Bam*HI and hybridized with radiolabeled 3′ *Plk2* probe, followed by autoradiography. The wild-type locus yielded a fragment of ~13 kbp, whereas the disrupted locus gave rise to a 6.8-kbp fragment, owing to a *Bam*HI site introduced by the Neo cassette. +/+, +/−, and −/−, $Plk2^{+/+}$, $Plk2^{+/-}$, and $Plk2^{-/-}$, respectively. (C) PCR analysis of the disrupted *Plk2* locus. PCRs were carried out with primers p1 to p3 and mouse tail DNA. Reaction mixtures were resolved on an agarose gel and stained with ethidium bromide. (D) Northern blot analysis showing the disruption of *Plk2* expression in $Plk2^{-/-}$ mice. On top is an autoradiograph showing detection with the 3′ *Plk2* probe of the full-length and a truncated (arrowhead) *Plk2* message in total RNA isolated from mouse brain. The controls were total RNA isolated from serum-starved NIH 3T3 cells (0h) or from cells stimulated with serum for 1 h (1h). The middle blot shows that the truncated *Plk2* message does not hybridize to the 5′ *Plk2* probe. The lower blot shows a methylene blue-stained membrane to demonstrate loading among the lanes. (E) Western blot analysis indicates the lack of Plk2 production in cultured embryonic fibroblasts. Cells were treated with nocodazole (M) and released into the cell cycle for 190 min (G_1). On top is a Western blot with a polyclonal antibody specific for the C terminus of Plk2. The arrow indicates the position of Plk2, and molecular mass markers (in kilodaltons) are shown on the left. Below is a Western blot with anti-Erk1 antibody to demonstrate loading in each lane.

trypsinized (0.25% trypsin, 1 mM EDTA; GIBCO BRL), washed with phosphate-buffered saline (PBS), and resuspended in PBS at a concentration of 1.2×10^7 per ml (0.9 ml total). After incubation with 25.2 μg of linearized replacement vector DNA for 5 min at 25°C, electroporation was performed with a 0.4-cm-gap-length cuvette and a Bio-Rad Gene Pulser set at 230 V and 500 μF. The cells were plated onto three 65-mm-diameter feeder plates. Geneticin (GIBCO BRL) was added to the medium to a final effective concentration of 260 μg/ml after 18 h, and 1-(2′-deoxy-2′-fluoro-β-D-arabinofuranosyl)-5-iodouracil was added to 0.2 μM after 40 h. Resistant ES cell clones were picked into 96-well plates covered with murine embryonic fibroblasts (MEFs). Cells that became 80% confluent were passed to and incubated in 24-well plates with MEFs. Subsequently, 75% of the cells from each well were frozen, and the rest were expanded on 12-well plates without MEFs to prepare DNA for analysis.

Generation of $Plk2^{-/-}$ mice. Four ES cell clones were injected into host blastocysts from MF1 outbreed mice (3), and lines 8H and 1D1 generated germ line chimeras, which were crossed with MF1 and 129/Sv mice. Intercrosses between heterozygous progeny of line 8H mice yielded wild-type, heterozygous, and $Plk2^{-/-}$ offspring in a ratio of 1:2:1, but intercrosses between line 1D1 progeny yielded almost no $Plk2^{-/-}$ offspring (data not shown). However, F_2 and F_3 crosses of line 1D1 progeny showed increased incidence of live $Plk2^{-/-}$ offspring (data not shown), suggesting that a "modifier" gene may be responsible for embryonic lethality in F_1 crosses in line 1D1. Therefore, the line 1D1 mouse was backcrossed twice with 129/Sv mice (Taconic), and intercrosses between the resultant heterozygotes showed a 1:2:1 distribution of wild-type, heterozygous, and $Plk2^{-/-}$ offspring (data not shown). The results reported here are consistent between line 8H and 1D1 mice.

Genotyping and analyses of *Plk2* expression. Genomic DNA was isolated from ES cells as described previously (43). Isolation of genomic DNA from clipped mouse tails was performed with a lysis buffer containing 100 mM Tris-HCl, pH 8.5, 5 mM EDTA, 0.2% sodium dodecyl sulfate, 200 mM NaCl, and 1 mg of proteinase K (GIBCO BRL)/ml. PCR analysis was performed with three primers: p1 (5′-ATGGAGCTCCTGCGGAC-3′), p2 (5′-GTCTGTGAAGCTCGATTTC-3′), and p3 (5′-ATATTGCTGAAGAGCTTGGCGGC-3′) (Fig. 1A). Cycling was for 45 s at 94°C, 1 min at 60°C, and 3 min at 72°C for 30 cycles with *Taq* DNA polymerase (Panvera). The PCR products were separated on 0.7% agarose gels and visualized by staining them with ethidium bromide. Southern and Northern blot analyses were performed using radiolabeled probes (Fig. 1A). The 5′ probe, corresponding to Met-1 to Lys-123, was generated by PCR with primers 5′-ATGGAGCTCCTGCGGAC-3′ and 5′-TCTTTTCCCTCTGATGAGG-3′, and the 3′ probe was the 1-kbp *Xba*I fragment from clone 2, corresponding to Leu-480 to Asn-682 (47). Total RNA was prepared from mouse brain using TRIZOL reagent (GIBCO BRL). Rapid amplification of cDNA ends by reverse transcription and PCR (RACE RT-PCR) analyses were performed according to the protocol for the 5′ RACE system (GIBCO BRL), except that cDNA was

purified by phenol extraction and ethanol precipitation. *Plk2*-specific cDNA was synthesized with primer 5′-TGCAGGAAGAAGTCATG-3′ and amplified by PCR with the Upstream Amplification Primer (GIBCO BRL) and 5′-GAATG GAGGTCTTCCTAGCAG-3′. Sequencing of the 5′ end of amplified cDNA was performed with primers 5′-CTGCCTGAGGTAGTATCG-3′ and 5′-TTCACA GCCGTGTCCTTG-3′. Western blot analysis of Plk2 in nocodazole-treated embryonic fibroblasts was performed as described previously (36).

Weight study and histological examination. To normalize the conditions for the weight study, a total of 10 to 12 newborns were kept with two nursing mice before they were weaned. Tail clipping was carried out on day 7 after birth, and the pups were weaned on the 18th day. Embryos and placentas were dissected out of decidua and cleared of membranes and umbilical cords in PBS. After excess buffer was blotted with a paper towel, they were weighed on a Mettler PG503-S balance. For histology, tissues were fixed in Bouin's solution for 24 to 40 h and embedded in paraffin. Sections (5 μm thick) were made with a Reichert-Jung Supercut 2050 microtome, and staining with hematoxylin and eosin was performed according to standard procedures.

TUNEL assays and immunohistochemistry. Tissues were fixed in 4% paraformaldehyde overnight at 4°C and embedded in paraffin to make 5-μm-thick sections. Terminal deoxynucleotidyltransferase-mediated dUTP-biotin nick end labeling (TUNEL) assays were performed with an ApopTag Red *In Situ* Detection kit (Serologicals Co.) according to the manufacturer's protocol. Immunohistochemistry with anti-phospho-histone H3 (Upstate Biotechnology) was carried out basically as described previously (59). Fluorescence confocal microscopy was performed as described previously (36). For cell counting, positive cells in each sample were justified with the area of the labyrinthine zone as calculated from hematoxylin- and eosin-stained sections.

Embryonic fibroblast cell culture and cell cycle analysis. Embryonic fibroblasts were derived from embryonic day 13.5 (E13.5) embryos as described previously (18). The cell suspension was plated onto one 15-cm-diameter tissue culture dish, and these were regarded as passage 1 cells. For cell cycle analysis, cells at passage 3 were incubated in Dulbecco's modified Eagle's medium plus 0.1% fetal bovine serum for 48 h. The cells were then incubated with normal growth medium and subjected to fluorescence-activated cell sorting (FACS) analysis as described previously (24). The study of cell proliferation over an extended time (48 h) was carried out using the protocol for studying 3T3 cell lines (54), except that 60-mm-diameter tissue culture plates were used.

RESULTS

Disruption of the *Plk2* locus. We constructed a gene replacement vector by replacing sequences encoding the conserved kinase domains I and II of *Plk2* with a DNA cassette conferring neomycin resistance (Neo) (Fig. 1A). The replacement vector was electroporated into ES cells, and subsequent selection and screening of 192 ES cell clones identified 4 clones with the desired disruption of the *Plk2* locus (Fig. 1B and C). Two independent lines of $Plk2^{+/-}$ mice were generated.

Northern blot analysis of total RNA isolated from adult $Plk2^{-/-}$ mouse brain with a 3′ *Plk2* probe detected a low-abundance RNA that is shorter than the full-length *Plk2* message (Fig. 1D, top). RACE RT-PCR was carried out to produce and amplify the 5′ ends of cDNAs from the total mRNA, and sequencing of the 5′ end with *Plk2*-specific probes revealed that the smaller RNA is indeed a truncated *Plk2* message containing, from 5′ to 3′, sequence from the Neo cassette, *Plk2* intron sequence immediately following the cassette, and sequence of the third exon of *Plk2* (data not shown). This truncated *Plk2* message did not hybridize to a 5′ *Plk2* probe that is upstream of the insertion site of the Neo cassette (Fig. 1D, middle). Therefore, the minor message appears to have originated from the Neo cassette, and it predicts a 59.2-kDa truncated Plk2 that does not have the first two kinase domains, including the conserved putative ATP-binding pocket that is necessary for Plk2 kinase activity (36). To examine whether any Plk2 is produced, fibroblasts derived from $Plk2^{-/-}$ embryos were treated with nocodazole, released into the cell cycle for 190 min, and analyzed by Western blotting with an antibody specific for the C terminus of Plk2. Our antibody failed to detect Plk2 in any tissue in wild-type animals; however, a prior study showed that the production of Plk2 in NIH 3T3 cells peaks at this time point (36). No full-length or truncated Plk2 was detected in $Plk2^{-/-}$ cells under these conditions (Fig. 1E). Altogether, these data suggest that our $Plk2^{-/-}$ mice are deficient in Plk2.

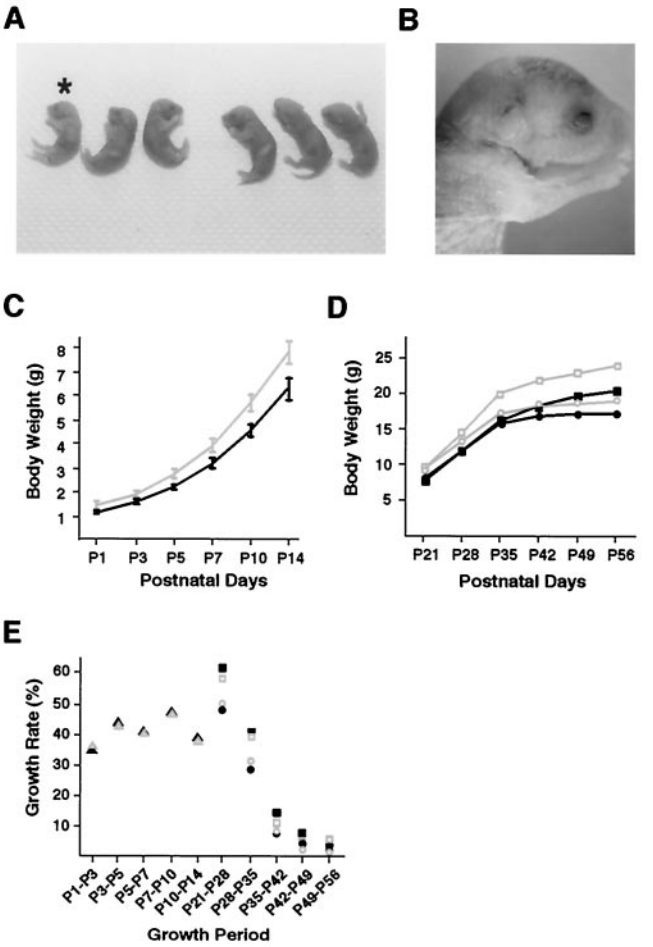

FIG. 2. Postnatal growth of $Plk2^{-/-}$ mice. (A) Newborn $Plk2^{-/-}$ mouse (asterisk) is small and pale. (B) Enlarged picture showing the incompletely closed eyelids of a newborn $Plk2^{-/-}$ mouse. (C and D) $Plk2^{-/-}$ and wild-type mice have similar growth curves. Males and females were weighed separately starting from postnatal day 21 (P21) (D). The shaded lines represent wild-type mice, and the solid lines represent $Plk2^{-/-}$ mice. The open and solid squares represent males, and the circles represent females. The error bars indicate standard deviations. (E) $Plk2^{-/-}$ and wild-type mice show similar growth rates. The growth rate was calculated by expressing the weight gain as a percentage of the initial weight for each specified growth period. The shaded symbols represent wild-type animals, and the solid symbols represent $Plk2^{-/-}$ mice. Triangles, male and female; squares, male; circles, female.

Growth of $Plk2^{-/-}$ mice. A summary of over 50 litters from heterozygous crosses showed that wild-type, heterozygous, and $Plk2^{-/-}$ mice were born at a ratio of 1:2:1, indicating that *Plk2* deletion did not cause embryonic lethality (data not shown).

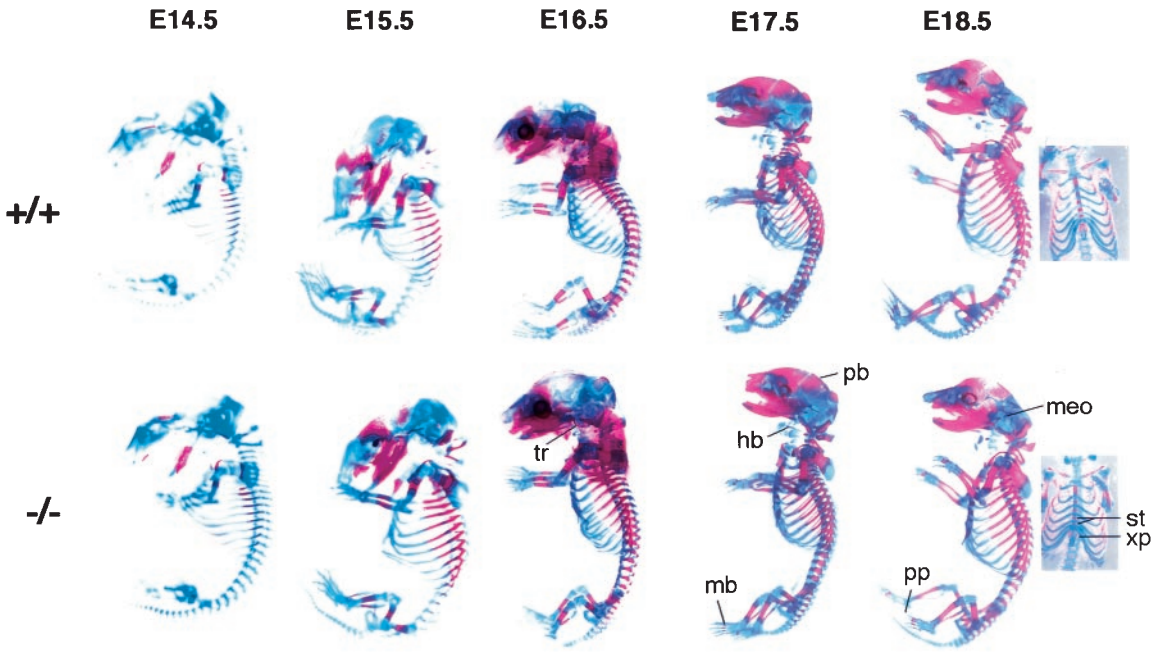

FIG. 3. Development of the skeleton in *Plk2*$^{-/-}$ embryos. Skeletal preparations from E14.5 to E18.5 embryos were stained with alcian blue and alizarin red. The ossification centers are stained red, and cartilage tissues are blue. Small embryos are enlarged to show details, so the sizes of the embryos on different embryonic days are not proportional. The labeled ossification centers are some of those that are indicative of the stage of skeletal development for the specified embryonic day (26). The insets at the right are ventral views of E18.5 skeletons showing delayed skeletal development in *Plk2*$^{-/-}$ embryos. tr, tympanic ring; pb, parietal bone; hb, cartilage primordium of body of hyoid bone; mb, metatarsal bones; meo, middle ear ossicles; pp, proximal phalanges; st, sternebrae; xp, upper region of xiphoid process.

However, *Plk2*$^{-/-}$ mice appeared smaller than other littermates, and their skin color was pale (Fig. 2A), although they did not appear to be anemic, because the color of their veins was similar to that in normal mice (Fig. 2A and B). About 30% of *Plk2*$^{-/-}$ mice were born with incompletely closed eyelids (Fig. 2B), but all *Plk2*$^{-/-}$ mice were viable. Adult *Plk2*$^{-/-}$ mice were fertile, with no anomaly detected in major tissues by histological examination (data not shown). Moreover, *Plk2*$^{-/-}$ and normal mice showed comparable 12-month survival rates (data not shown).

We monitored the growth of *Plk2*$^{-/-}$ mice. *Plk2*$^{-/-}$ newborns were, with no exception, the smallest in the litter, on average ~20% smaller than normal mice ($0.05 < P < 0.1$) (Fig. 2C). Starting from the third week, about the time when growth hormone takes effect, the weights of female and male mice were analyzed separately because their growth rates began to differ (13). The results showed that *Plk2*$^{-/-}$ mice were consistently smaller than normal mice (Fig. 2D). Comparison of weight gains shows that normal and *Plk2*$^{-/-}$ mice have practically the same growth rate (Fig. 2E), indicating that *Plk2* is not required for postnatal growth and that the dwarfism of *Plk2*$^{-/-}$ mice is likely caused by defective embryonic development.

Development of *Plk2*$^{-/-}$ embryos. To investigate whether disruption of *Plk2* affected the overall progress of embryonic development, skeletal development was examined by staining with alcian blue and alizarin red. Bone development in the mouse follows an orderly progression, in which proliferating

TABLE 1. Growth of the placenta and embryo

Genotype[a]	Mean wt (g) ± SD (no. measured) at:			
	E15.5	E16.5	E17.5	E18.5
Embryos				
+/+	0.382 ± 0.046 (6)	0.575 ± 0.080 (11)	0.059 ± 0.111 (5)	1.229 ± 0.049 (6)
+/−	0.356 ± 0.065 (7)	0.574 ± 0.076 (30)	0.984 ± 0.045 (6)	1.177 ± 0.067 (8)
−/−	0.382 ± 0.070 (4)	0.538 ± 0.077 (13)	0.902 ± 0.066 (3)	1.061 ± 0.091 (4)
Placentas				
+/+	NA[b]	0.065 ± 0.005 (11)	0.080 ± 0.008 (5)	0.057 ± 0.004 (4)
+/−	NA	0.062 ± 0.007 (26)	0.078 ± 0.009 (6)	0.059 ± 0.005 (5)
−/−	NA	0.045 ± 0.006 (10)	0.059 ± 0.005 (3)	0.042 ± 0.003 (3)

[a] +/+, *plk2*$^{+/+}$; +/−, *Plk2*$^{+/-}$; −/−, *Plk2*$^{-/-}$.
[b] NA, not analyzed.

chondrocytes gradually differentiate into hypertrophic cells (56). Proliferating chondrocytes can be stained with alcian blue, and differentiated mature hypertrophic cells are stained with alizarin red (56). We compared the first appearance of ossification centers, which were stained red, at each stage in wild-type and *Plk2*$^{-/-}$ embryos and with those documented by Kaufman (26). The results showed that ossification occurred at the same time in most bones in *Plk2*$^{-/-}$ and normal embryos (Fig. 3). However, ossification on the third and fourth sternebrae and in the upper region of the xiphoid process was less advanced in all three *Plk2*$^{-/-}$ embryos from two litters. These data suggest that the *Plk2* deletion did not significantly disrupt the overall development of the embryo.

On the other hand, *Plk2*$^{-/-}$ embryos were ~94% of the weight of normal embryos at E16.5 and E17.5 and reached 86% at E18.5 ($P < 0.05$) (Table 1), suggesting a role for *Plk2* in embryonic growth. Assessing the growth of the placenta showed that the average weight of placentas of *Plk2*$^{-/-}$ embryos was ~70% ($P < 0.05$) of that of placentas of normal embryos at E16.5, and this difference was maintained until birth (Table 1). Mouse placenta is composed of a maternal (decidual) component and a component of embryonic origin, including a spongy layer of trophoblast cells, the labyrinth, and the chorionic plate. As the placenta matures, the labyrinthine zone increases in volume from E12.0 to E17.5 due to cell proliferation in the region and thereafter remains unchanged until birth (26). Histological analysis of placentas at E18.5 indicated that the labyrinthine zone of *Plk2*$^{-/-}$ embryos was significantly smaller than that of normal embryos, but the overall organization and structure, including the size of cells in this region, appeared to be normal (Fig. 4A). Because the size of the labyrinthine zone can be affected by cell death (apoptosis) and cell proliferation in the region, we used a TUNEL assay to assess cell death and phospho-histone H3 staining for cells in mitosis as an index for cell proliferation. The results showed no significant difference in the number of apoptotic cells per square millimeter in the labyrinthine zones of the placentas of normal and *Plk2*$^{-/-}$ embryos (Fig. 4B). On the other hand, the number of cells per square millimeter stained for phospho-histone H3 in the labyrinthine zones of *Plk2*$^{-/-}$ embryos was ~64% of that in *Plk2*$^{+/-}$ embryos ($P < 0.05$) (Fig. 4C). These results provide evidence that *Plk2* is involved in cell proliferation in vivo.

Cell cycle progression of *Plk2*$^{-/-}$ embryonic fibroblasts cultured in vitro. We further investigated the role of *Plk2* in cell proliferation with cultured fibroblasts prepared from E13.5 embryos. Cells seeded at high density were incubated for 48 h, and the cells were counted. In early passages (passages 3 to 5), the count was greater for *Plk2*$^{+/+}$ and *Plk2*$^{+/-}$ cells than for *Plk2*$^{-/-}$ cells ($P < 0.05$) (Fig. 5A). On average, *Plk2*$^{+/+}$ and *Plk2*$^{+/-}$ fibroblasts divided in ~22 h, whereas *Plk2*$^{-/-}$ cells divided in ~25 h. Thus, the cell cycle appears to be slightly delayed in the absence of Plk2. At passage 6, however, fibroblasts from both sources began to divide at about the same rate, perhaps because they reached the crisis stage. These results suggest a role for *Plk2* in the cell cycle.

To investigate how cell cycle progression is affected by *Plk2* deletion, cells from passage 3 were incubated in 0.1% serum for 48 h. FACS analysis of DNA content showed that 12 h after serum stimulation, more *Plk2*$^{+/-}$ cells than *Plk2*$^{-/-}$ cells were

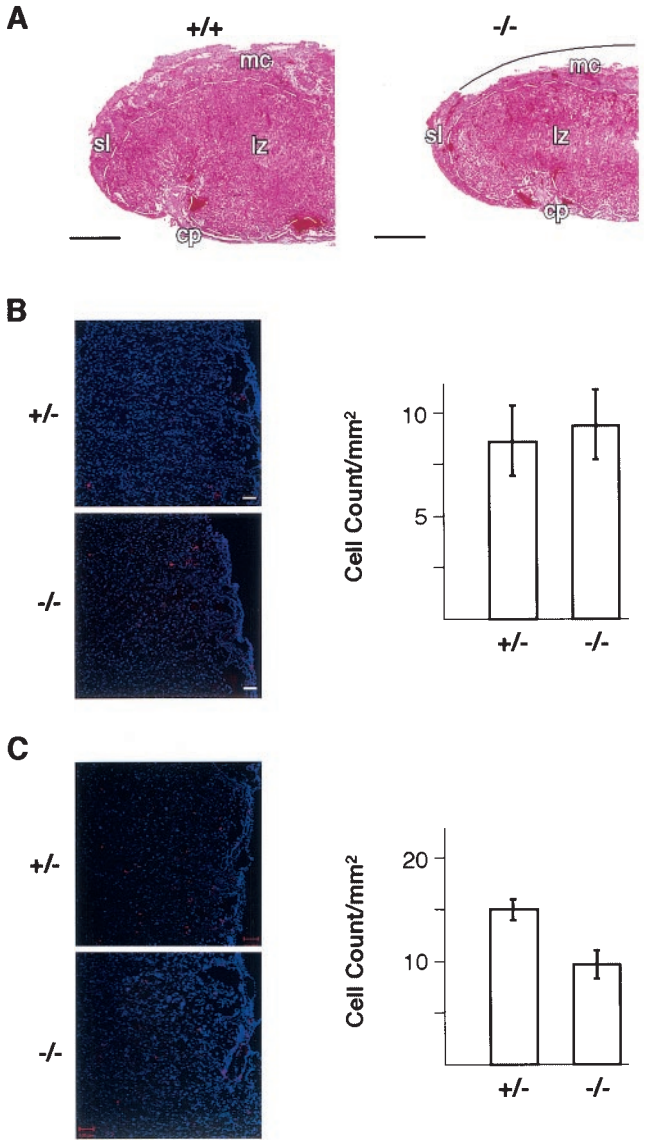

FIG. 4. Analysis of the placentas of *Plk2*$^{-/-}$ embryos. (A) Hematoxylin- and eosin-stained section of half of a placenta showing diminished labyrinthine zone, indicated by white dashed lines, in *Plk2*$^{-/-}$ (−/−) embryos. The curved solid line depicts a portion of the maternal component that was peeled off during sample preparation. mc, maternal (decidual) component; sl, spongiotrophoblast layer at periphery of the placenta; lz, labyrinthine zone; cp, chorionic plate. +/+, *Plk2*$^{+/+}$. Bar, 0.5 mm. (B) The labyrinthine zones of *Plk2*$^{+/-}$ (+/−) and *Plk2*$^{-/-}$ embryos contain similar numbers of apoptotic cells. On the left are fluorescence confocal microscopy images of TUNEL-stained (red) placenta sections. Cell nuclei were stained with DAPI (4′,6′-diamidino-2-phenylindole) (blue). On the right, counts of TUNEL-stained cells from five samples are summarized. The error bars indicate standard deviations. (C) Phospho-histone H3 staining shows that fewer cells are proliferating in the labyrinthine zone of the placenta of *Plk2*$^{-/-}$ embryos than in *Plk2*$^{+/-}$ embryos. On the left, fluoresence confocal microscopy images of sections of the labyrinthine zone are shown. Phospho-histone H3-positive cells are stained red, and cell nuclei are blue. On the right, counts of phospho-histone H3-positive cells from five tissue sections are summarized. The results are representative of two independent experiments.

in S phase (Fig. 5B). Results from two independent experiments showed an increase in the S-phase population in $Plk2^{+/-}$ cells at 12 h compared to $Plk2^{-/-}$ cells. As a result, 21.64% of $Plk2^{+/-}$ cells were in S phase compared with 11.83% for $Plk2^{-/-}$ cells at the same time point (Fig. 5C), suggesting a delay for $Plk2^{-/-}$ cells in entering S phase. These data suggest that *Plk2* may influence G_1 progression, but unlike *Plk1*, it is not required for cell division.

DISCUSSION

Our studies of $Plk2^{-/-}$ mice reveal a role for *Plk2* in embryonic development. Growth retardation of $Plk2^{-/-}$ embryos and a slight delay in the development of the skeleton were observed late in gestation, whereas diminished weight of the placentas of $Plk2^{-/-}$ embryos was detected as early as E16.5. Immunohistochemistry analyses of cells in the labyrinthine zone indicated that fewer proliferating cells are present in $Plk2^{-/-}$ embryos than in normal embryos, resulting in a reduced labyrinthine zone. This raises the possibility that the phenotypes observed in embryonic growth and skeletal development are caused by impaired trophic function of the placenta, although a direct role for *Plk2* cannot be ruled out. Our data have uncovered a role for *Plk2* in cell proliferation in vivo but cannot pinpoint the precise time of manifestation of growth retardation, as this requires surveying a large number of embryos, because even embryos in the same litter vary significantly in development (26). Disruption of other genes involved in the regulation of cell proliferation leads to changes in animal growth. For example, cyclin D1 knockout mice showed growth retardation, whereas mutation of the negative regulator $p27^{Kip1}$ resulted in enhanced growth (14, 16, 28, 37, 46).

On the other hand, $Plk2^{-/-}$ mice have a growth rate comparable to that of normal mice, indicating that *Plk2* is not required for postnatal growth. This is consistent with the results of a previous study showing that *Plk2* message is generally absent from tissues of the adult mouse except in the brain and lung (47). The only other example we are aware of is the fact that the disruption of the gene encoding insulin-like growth factor II (IGF-II) exclusively affects embryonic growth (8). However, IGF-II exerts its effect early (E11.0), and the mutant mice are severely growth retarded at birth (60% of normal weight) (8).

Cell cycle analysis of cultured $Plk2^{-/-}$ embryonic fibroblasts indicates that these cells proliferate more slowly than cells expressing *Plk2* and have delayed entry into S phase from G_1. These results suggest a role for *Plk2* in the cell cycle. *Plk2* expression is limited to early G_1 (36, 47), and Cdc25A is expressed in G_1 and required for progression from G_1 into S phase (21, 25). It is possible that Plk2 contributes to Cdc25A activation, but it is clearly not required. A previous study showed that overexpression of Plk2 induces changes in cell morphology and that *Plk2* is expressed during the time when rounded cells are flattening and spreading after mitosis, which prompted speculation that *Plk2* may be involved in these processes, as it can localize to the microtubule organizing center (36). Changes in the microtubule cytoskeleton appear to be necessary for cells to progress from G_1 to S phase, as microtubule stabilization by taxol inhibits the initiation of DNA synthesis whereas microtubule depolymerization seems to prompt DNA synthesis (6, 7). However, primary $Plk2^{-/-}$ fibroblasts showed no significant change in cell morphology (data not shown) and were able to complete the cell cycle. Embryonic fibroblasts lacking cyclin D1 had a completely normal cell cycle, despite the fact that cyclin D1 knockout mice were small (14). Interestingly, knockin of cyclin E to replace the coding sequence of cyclin D1 completely rescued all phenotypes of cyclin D1 deletion (17). In mammalian cells, Plk2 and Plk3 show overlapping expression and cellular localiza-

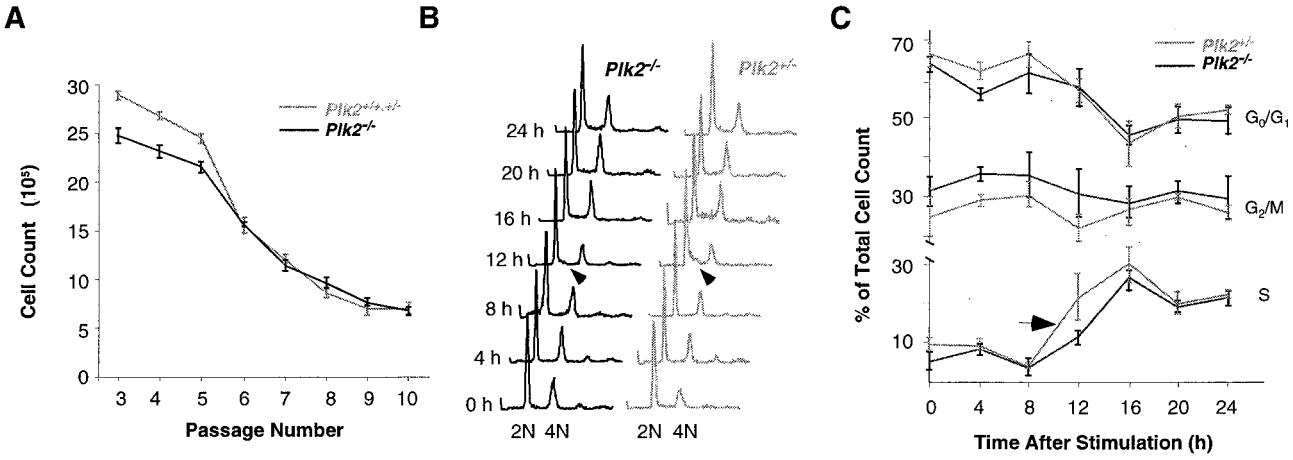

FIG. 5. Analysis of proliferation of cultured embryonic fibroblasts. (A) Cell proliferation assays. The cells were counted after 48 h of incubation. Values were calculated from one $Plk2^{+/+}$, two $Plk2^{+/-}$, and three $Plk2^{-/-}$ cell lines derived from a single litter. The results are representative of three independent experiments. The error bars indicate standard deviations. (B) FACS analysis of cell cycle progression after serum stimulation. Times after serum stimulation are shown on the left, and G_1 (2N) and G_2/M (4N) cell populations are indicated. The arrowheads point to differences between the S-phase cell populations in $Plk2^{-/-}$ and $Plk2^{+/-}$ cells. (C) Summary of FACS analyses of five $Plk2^{-/-}$ and three $Plk2^{+/-}$ cell lines from two independent experiments. A rapid increase in the S-phase cell population in $Plk2^{+/-}$ cells from 8 to 12 h after serum stimulation is indicated by an arrow.

tion in G_1 (4, 36, 57), and it is possible that Plk3 functions to complement Plk2 in *Plk2*$^{-/-}$ cells.

ACKNOWLEDGMENTS

We thank Philip Leder for the gift of TC1 ES cells. We are grateful to Andrew and Jill McMahon for valuable suggestions and permission to use their facilities. Technical expertise provided by Fanxin Long and Diane Faria is greatly appreciated. We are also indebted to Thomas Benjamin, John Carroll, and Ron Brownson for histological analysis of tissues of adult mice. Critical reading and editing of the manuscript by Eleanor Erikson are highly appreciated.

This work is supported by a grant from the National Institutes of Health (GM59172) to R.L.E.

REFERENCES

1. **Alexandru, G., F. Uhlmann, K. Mechtler, M. A. Poupart, and K. Nasmyth.** 2001. Phosphorylation of the cohesin subunit Scc1 by Polo/Cdc5 kinase regulates sister chromatid separation in yeast. Cell **105:**459–472.
2. **Carmena, M., M. G. Riparbelli, G. Minestrini, A. M. Tavares, R. Adams, G. Callaini, and D. M. Glover.** 1998. *Drosophila* polo kinase is required for cytokinesis. J. Cell Biol. **143:**659–671.
3. **Charron, J., B. A. Malynn, P. Fisher, V. Stewart, L. Jeannotte, S. P. Goff, E. J. Robertson, and F. W. Alt.** 1992. Embryonic lethality in mice homozygous for a targeted disruption of the N-myc gene. Genes Dev. **6:**2248–2257.
4. **Chase, D., Y. Feng, B. Hanshew, J. A. Winkles, D. L. Longo, and D. K. Ferris.** 1998. Expression and phosphorylation of fibroblast-growth-factor-inducible kinase (Fnk) during cell-cycle progression. Biochem. J. **333:**655–660.
5. **Conn, C. W., R. F. Hennigan, W. Dai, Y. Sanchez, and P. J. Stambrook.** 2000. Incomplete cytokinesis and induction of apoptosis by overexpression of the mammalian polo-like kinase, Plk3. Cancer Res. **60:**6826–6831.
6. **Crossin, K. L., and D. H. Carney.** 1981. Evidence that microtubule depolymerization early in the cell cycle is sufficient to initiate DNA synthesis. Cell **23:**61–71.
7. **Crossin, K. L., and D. H. Carney.** 1981. Microtubule stabilization by taxol inhibits initiation of DNA synthesis by thrombin and by epidermal growth factor. Cell **2:**341–350.
8. **DeChiara, T. M., A. Efstratiadis, and E. J. Robertson.** 1990. A growth-deficiency phenotype in heterozygous mice carrying an insulin-like growth factor II gene disrupted by targeting. Nature **345:**78–80.
9. **Descombes, P., and E. A. Nigg.** 1998. The polo-like kinase Plx1 is required for M phase exit and destruction of mitotic regulators in *Xenopus* egg extracts. EMBO J. **17:**1328–1335.
10. **do Carmo Avides, M., A. Tavares, and D. M. Glover.** 2001. Polo kinase and Asp are needed to promote the mitotic organizing activity of centrosomes. Nat. Cell Biol. **3:**421–424.
11. **Donohue, P. J., G. F. Alberts, Y. Guo, and J. A. Winkles.** 1995. Identification by targeted differential display of an immediate early gene encoding a putative serine/threonine kinase. J. Biol. Chem. **270:**10351–10357.
12. **Duncan, P. I., N. Pollet, C. Niehrs, and E. A. Nigg.** 2001. Cloning and characterization of Plx2 and Plx3, two additional Polo-like kinases from *Xenopus laevis.* Exp. Cell Res. **270:**78–87.
13. **Efstratiadis, A.** 1998. Genetics of mouse growth. Int. J. Dev. Biol. **42:**955–976.
14. **Fantl, V., G. Stamp, A. Andrews, I. Rosewell, and C. Dickson.** 1995. Mice lacking cyclin D1 are small and show defects in eye and mammary gland development. Genes Dev. **9:**2364–2372.
15. **Feng, Y., D. L. Longo, and D. K. Ferris.** 2001. Polo-like kinase interacts with proteasomes and regulates their activity. Cell Growth Differ. **12:**29–37.
16. **Fero, M. L., M. Rivkin, M. Tasch, P. Porter, C. E. Carow, E. Firpo, K. Polyak, L.-H. Tsai, V. Broudy, R. M. Perlmutter, K. Kaushansky, and J. M. Roberts.** 1996. A syndrome of multiorgan hyperplasia with features of gigantism, tumorigenesis, and female sterility in p27^{Kip1}-deficient mice. Cell **85:**733–744.
17. **Geng, Y., W. Whoriskey, M. Y. Park, R. T. Bronson, R. H. Medema, T. Li, R. A. Weinberg, and P. Sicinski.** 1999. Rescue of cyclin D1 deficiency by knockin cyclin E. Cell **97:**767–777.
18. **Giroux, S., M. Tremblay, D. Bernard, J. F. Cardin-Girard, S. Aubry, L. Larouche, S. Rousseau, J. Huot, J. Landry, L. Jeannotte, and J. Charron.** 1999. Embryonic death of Mek1-deficient mice reveals a role for this kinase in angiogenesis in the labyrinthine region of the placenta. Curr. Biol. **9:**369–372.
19. **Golsteyn, R. M., H. A. Lane, K. E. Mundt, L. Arnaud, and E. A. Nigg.** 1996. The family of polo-like kinases, p. 107–114. *In* L. Meijer, S. Guidet, and L. Vogel (ed.), Progress in cell cycle research, vol. 2. Plenum Press, New York, N.Y.
20. **Hardy, C. F. J., and A. Pautz.** 1996. A novel role for Cdc5p in DNA replication. Mol. Cell. Biol. **16:**6775–6782.
21. **Hoffman, I., G. Draetta, and E. Karsenti.** 1994. Activation of the phosphatase activity of human cdc25A by a cdk2-cyclin E dependent phosphorylation at the G1/S transition. EMBO J. **13:**4302–4310.
22. **Holtrich, U., G. Wolf, J. Yuan, J. Bereiter-Hahn, T. Karn, M. Weiler, G. Kauselmann, M. Rehli, R. Andreesen, M. Kaufmann, D. Kuhl, and K. Strebhardt.** 2000. Adhesion induced expression of the serine/threonine kinase Fnk in human macrophages. Oncogene **19:**4832–4839.
23. **Hu, F., Y. Wang, D. Liu, Y. Li, J. Oin, and S. J. Elledge.** 2001. Regulation of the Bub2/Bfa1 GAP complex by Cdc5 and cell cycle checkpoints. Cell **107:**655–665.
24. **Jang, Y. J., S. Ma, Y. Terada, and R. L. Erikson.** 2002. Phosphorylation of threonine-210 and the role of serine-137 in the regulation of mammalian polo-like kinase. J. Biol. Chem. **277:**44115–44120.
25. **Jinno, S., K. Suto, A. Nagata, M. Igarashi, Y. Kanaoka, H. Nojima, and H. Okayama.** 1994. Cdc25A is a novel phosphatase functioning early in the cell cycle. EMBO J. **13:**1549–1556.
26. **Kaufman, M. H.** 1992. The atlas of mouse development. Academic Press Ltd., London, United Kingdom.
27. **Kauselmann, G., M. Weiler, P. Wulff, S. Jessberger, U. Konietzko, J. Scafidi, U. Staubli, J. Bereiter-Hahn, K. Strebhardt, and D. Kuhl.** 1999. The polo-like protein kinases Fnk and Snk associate with a Ca^{2+}- and integrin-binding protein and are regulated dynamically with synaptic plasticity. EMBO J. **18:**5528–5539.
28. **Kiyokawa, H., R. D. Kineman, K. O. Manova-Todorova, V. C. Soares, E. S. Hoffman, M. Ono, D. Khanam, A. C. Hayday, L. A. Frohman, and A. Koff.** 1996. Enhanced growth of mice lacking the cyclin-dependent kinase inhibitor function of p27^{Kip1}. Cell **85:**721–732.
29. **Kotani, S., S. Tugendreich, M. Fujii, P.-M. Jorgensen, N. Watanabe, C. Hoog, P. Hieter, and K. Todokoro.** 1998. PKA and MPF-activated polo-like kinase regulate anaphase-promoting complex activity and mitosis progression. Mol. Cell **1:**371–380.
30. **Kumagai, A., and W. G. Dunphy.** 1996. Purification and molecular cloning of Plx1, a Cdc25-regulatory kinase from *Xenopus* egg extracts. Science **273:**1377–1380.
31. **Lane, H., and E. A. Nigg.** 1997. Cell-cycle control: POLO-like kinases join the outer circle. Trends Cell. Biol. **7:**63–68.
32. **Lane, H. A., and E. A. Nigg.** 1996. Antibody microinjection reveals an essential role for human polo-like kinase 1 (Plk1) in the functional maturation of mitotic centrosomes. J. Cell Biol. **135:**1701–1713.
33. **Lee, K. S., and R. L. Erikson.** 1997. Plk is a functional homolog of *Saccharomyces cerevisiae* Cdc5, and elevated Plk activity induces multiple septation structures. Mol. Cell. Biol. **17:**3408–3417.
34. **Lin, C. Y., M. L. Madsen, F. R. Yarm, Y. J. Jang, X. Liu, and R. L. Erikson.** 2000. Peripheral Golgi protein GRASP65 is a target of mitotic polo-like kinase (Plk) and Cdc2. Proc. Natl. Acad. Sci. USA **97:**12589–12594.
35. **Liu, X., and R. L. Erikson.** 2002. Activation of Cdc2/cyclin B and inhibition of centrosome amplification in cells depleted of Plk1 by siRNA. Proc. Natl. Acad. Sci. USA **99:**8672–8676.
36. **Ma, S., M.-Y. Liu, Y.-L. O. Yuan, and R. L. Erikson.** 2003. The serum-inducible kinase is a G1 polo-like kinase that is inhibited by the calcium- and integrin-binding protein CIB. Mol. Cancer Res. **1:**376–384.
37. **Nakayama, K., N. Ishida, M. Shirane, A. Inomata, T. Inoue, N. Shishido, I. Horii, D. Y. Loh, and K.-I. Nakayama.** 1996. Mice lacking p27^{kip1} display increased body size, multiple organ hyperplasia, retinal dysplasia, and pituitary tumors. Cell **85:**707–720.
38. **Ohkura, H., I. M. Hagan, and D. M. Glover.** 1995. The conserved *Schizosaccharomyces pombe* kinase plo1, required to form a bipolar spindle, the actin ring, and septum, can drive septum formation in G1 and G2 cells. Genes Dev. **9:**1059–1073.
39. **Ouyang, B., H. Pan, L. Lu, J. Li, P. Stambrook, B. Li, and W. Dai.** 1997. Human Prk is a conserved protein serine/threonine kinase involved in regulating M phase functions. J. Biol. Chem. **272:**28646–28651.
40. **Qian, Y.-W., E. Erikson, C. Li, and J. L. Maller.** 1998. Activated polo-like kinase Plx1 is required at multiple points during mitosis in *Xenopus laevis.* Mol. Cell. Biol. **18:**4262–4271.
41. **Qian, Y.-W., E. Erikson, and J. L. Maller.** 1999. Mitotic effects of a constitutively active mutant of the *Xenopus* polo-like kinase Plx1. Mol. Cell. Biol. **19:**8625–8632.
42. **Qian, Y. W., E. Erikson, F. E. Taieb, and J. L. Maller.** 2001. The polo-like kinase Plx1 is required for activation of the phosphatase Cdc25C and cyclin B-Cdc2 in *Xenopus* oocytes. Mol. Biol. Cell. **12:**1791–1799.
43. **Ramirez-Solis, R., A. C. Davis, and A. Bradley.** 1993. Gene targeting in embryonic stem cells. Methods Enzymol. **225:**855–878.
44. **Sanchez, Y., J. Bachant, H. Wang, F. Hu, D. Liu, M. Tetzlaff, and S. J. Elledge.** 1999. Control of the DNA damage checkpoint by chk1 and rad53 protein kinases through distinct mechanisms. Science **286:**1166–1171.
45. **Shirayama, M., W. Zachariae, R. Ciosk, and K. Nasmyth.** 1998. The Polo-like kinase Cdc5p and the WD-repeat protein Cdc20p/fizzy are regulators and substrates of the anaphase promoting complex in *Saccharomyces cerevisiae.* EMBO J. **17:**1336–1349.
46. **Sicinski, P., J. L. Donaher, S. B. Parker, T. Li, A. Fazeli, G. Humphrey, S. Z. Haslam, R. T. Bronson, S. J. Elledge, and R. A. Weinberg.** 1995. Cyclin D1

provides a link between development and oncogenesis in the retina and breast. Cell **82:**621–630.
47. **Simmons, D. L., B. G. Neel, R. Stevens, G. Evett, and R. L. Erikson.** 1992. Identification of an early-growth-response gene encoding a novel putative protein kinase. Mol. Cell. Biol. **12:**4164–4169.
48. **Smits, V. A., R. Klompmaker, L. Arnaud, G. Rijksen, E. A. Nigg, and R. H. Medema.** 2000. Polo-like kinase-1 is a target of the DNA damage checkpoint. Nat. Cell Biol. **2:**672–676.
49. **Song, S., and K. S. Lee.** 2001. A novel function of *Saccharomyces cerevisiae* CDC5 in cytokinesis. J. Cell Biol. **152:**451–470.
50. **Sumara, I., E. Vorlaufer, P. T. Stukenberg, O. Kelm, N. Redemann, E. A. Nigg, and J. M. Peters.** 2002. The dissociation of cohesin from chromosomes in prophase is regulated by polo-like kinase. Mol. Cell **9:**515–525.
51. **Sunkel, C. L., and D. M. Glover.** 1988. *polo*, a mitotic mutant of *Drosophila* displaying abnormal spindle poles. J. Cell Sci. **89:**25–38.
52. **Sutterlin, C., C. Y. Lin, Y. Feng, D. K. Ferris, R. L. Erikson, and V. Malhotra.** 2001. Polo-like kinase is required for the fragmentation of pericentriolar Golgi stacks during mitosis. Proc. Natl. Acad. Sci. USA **98:**9128–9132.
53. **Toczyski, D. P., D. J. Galgoczy, and L. H. Hartwell.** 1997. CDC5 and CKII control adaptation to the yeast DNA damage checkpoint. Cell **90:**1097–1106.
54. **Todaro, G. J., and H. Green.** 1963. Quantitative studies of the growth of mouse embryo cells in culture and their development into established lines. J. Cell Biol. **17:**299–313.
55. **Toyoshima-Morimoto, F., E. Taniguchi, N. Shinya, A. Iwamatsu, and E. Nishida.** 2001. Polo-like kinase 1 phosphorylates cyclin B1 and targets it to the nucleus during prophase. Nature **410:**215–220.
56. **Vortkamp, A., K. S. Lee, B. Lanske, G. V. Serge, H. M. Kronenberg, and C. J. Tabin.** 1996. Regulation of rate of cartilage differentiation by Indian Hedgehog and PTH-related protein. Science **273:**613–621.
57. **Wang, O., S. Xie, J. Chen, K. Fukasawa, U. Naik, F. Traganos, Z. Darzynkiewicz, M. Jhanwar-Unival, and W. Dai.** 2002. Cell cycle arrest and apoptosis induced by human Polo-like kinase 3 is mediated through perturbation of microtubule integrity. Mol. Biol. Cell. **22:**3450–3459.
58. **Xie, S., H. Wu, Q. Wang, J. P. Cogswell, I. Husain, C. Conn, P. Stambrook, M. Jhanwar-Uniyal, and W. Dai.** 2001. Plk3 functionally links DNA damage to cell cycle arrest and apoptosis at least in part via the p53 pathway. J. Biol. Chem. **276:**43305–43312.
59. **Yu, J., T. J. Carrol, and A. P. McMahon.** 2002. Sonic hedgehog regulates proliferation and differentiation of mesenchymal cells in the mouse metanephric kidney. Development **129:**5301–5312.